Pis'ma v ZhETF, vol. 102, iss. 5, pp. 348 – 353

Generation of THz radiation by AlGaAs nanowires

V. N. Trukhin[+*1)], A. S. Buyskih[+], A. D. Bouravlev[+×°], I. A. Mustafin[+*], Yu. B. Samsonenko[×], A. V. Trukhin[+°], G. E. Cirlin[+×°□], M. A. Kaliteevski[+×], D. A. Zeze[▽], A. J. Gallant[▽]

[+]*Ioffe Physicotechnical Institute of the RAS, 194021 St.-Petersburg, Russia*

[*] *St.-Petersburg National Research University of Information Technologies, Mechanics and Optics, 197101 St.-Petersburg, Russia*

[×]*St.-Petersburg Academic University of the RAS, 194021 St.-Petersburg, Russia*

[°]*St.-Petersburg State University, 199034 St.-Petersburg, Russia*

[▽]*School Engineering and Computing Sciences, Durham University, South Road, DH1 3LE Durham, UK*

[□]*St.-Peterburg Polytechnic University, 195251 St.-Peterburg, Russia*

Submitted 15 July 2015
Resubmitted 22 July 2015

Terahertz (THz) emission by AlGaAs nanowires grown on a GaAs substrate under excitation by femtosecond optical pulses has been observed. It is demonstrated that THz emission occurs via excitation of photocurrent in the nanowires. The dynamics of photoinduced charge carriers is studied via the influence of an electron-hole plasma on THz radiation. It is shown that the capture of charge carriers on vacancies which exist at the boundaries of nanowires, on the interfaces between cubic and hexagonal phase in nanowires, leads to an increase in the efficiency of THz emission.

DOI: 10.7868/S0370274X15170129

Semiconductor nanowires (NWs) have attracted substantial interest in the past decade due to their unique properties, making possible a wide range of applications in nanophotonics, nanoelectronics, and bioelectronics [1–3]. Another prospective application of NWs is in the generation of THz radiation. Recent experimental results have shown that the efficiency of THz emission can be substantially increased if the bulk material of the emitter is replaced by a structured surface [4–9]. Initial experimental studies of THz emission from InAs [7] and GaAs [8] NW arrays, excited by femtosecond laser pulses, demonstrated that the efficiency of THz generation can be increased by a factor of 15 when compared to bulk materials after accounting for the NW fill factor. Furthermore, since the efficiency of the THz emission is defined by concentration and mobility of charge carriers, studies of THz emission can be used to determine the transport, relaxation and recombination properties of electrons and holes in nanowires.

At present, it is commonly assumed that two kinds of physical processes are involved in the generation of THz radiation in semiconductors which are excited by short optical pulses: i) the motion of photoinduced charge carriers in the vicinity of surface [10, 11]; and ii) the nonlinear optical processes (optical rectification) [12].

Photoinduced current can be caused by a number of factors: i) built-in surface electric field or a biased electric field (in this case, THz generation is defined by the drift current) [13, 14]; ii) ambipolar diffusion at nonuniform excitation (THz radiation is generated by diffusion current) [15] or iii) anisotropy in the momentum distribution of charge carriers [16]. The current paper is aimed at the investigation of THz emission from AlGaAs nanowires excited by femtosecond laser pulses.

Nanowires with the average composition $Al_{0.2}Ga_{0.8}As$ were grown by the VLS method [17] on (111)B oriented GaAs substrates using an MBE EP 1203 system equipped with Ga, Al, As, and Au solid state sources. The chosen process parameters provided growth of NWs perpendicular to surface of substrate, as shown in Fig. 1a.

For the growth process, first, the substrate was annealed to remove the oxide from the surface onto which a 250 nm thick buffer layer of GaAs was grown. On top of the buffer layer, a 0.2 nm thick Au layer was deposited. Deposition of the material was stopped for 1 minute during which time the Au layer decomposes into droplets. Subsequently, the AlGaAs NWs were grown under the Au droplets which act as a catalyst in the VLS process.

[1)]e-mail: valera.truchin@mail.ioffe.ru

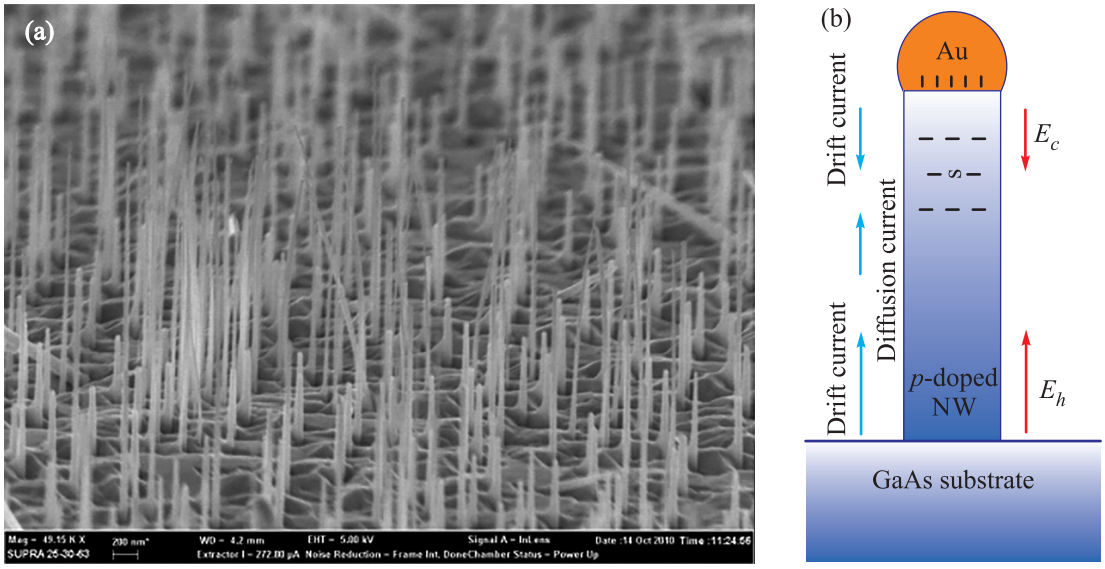

Fig. 1. (Color online) (a) – SEM image of the sample. (b) – The scheme of photocurrent in the sample

The resulting NWs have diameters of approximately 60 nm with a length of 1 μm and a fill factor of about 1.5 %. As is also the case with intentionally undoped material during MBE growth, the NWs have slight p-type conductivity. At the interface between Au cap and the NW, a Schottky barrier occurs, as shown in Fig. 1b. Note that in the case of a p-doped NW, the electric field of Schottky barrier E_c is directed towards a substrate. In turn, the electric field E_h of heterojunction between NW and GaAs substrate is opposite to the direction of Schottky barrier electric field (see Fig. 1b).

Optical excitation of the sample was provided using a pulsed Ti:Sapphire laser with pulse duration 90 fs and repetition rate 80 MHz. The central wavelength of the radiation was tuned in the range from 690 nm to 920 nm. Terahertz (THz) radiation was detected by electro-optic sampling or a Golay cell which was screened from stray infrared radiation by black polyethylene. The sample was illuminated at an oblique incidence, and THz radiation was collected in mirror geometry [9]. The THz detector was oriented at the same angle as incidence angle.

Studies of the dependence of THz power on incidence angle and also optical excitation wavelength were carried out in order to analyze the generation process. The dynamics of non-equilibrium carriers were studied by optical-pump terahertz generation-probe time-domain spectroscopy [9]. The sample was illuminated by two optical pulses, and the average THz power was measured as a function of the delay between the pulses which were produced by beam splitting one initial pulse. The first pulse generates an electron-hole plasma in the sample. The second pulse was modulated with frequency 12 Hz. The output signal of the THz detector (a Golay cell) was measured by a lock-in amplifier, synchronized with the modulation frequency. The intensity of the second pulse was chosen to be within the linear response range, i.e. when amplitude of THz radiation is linearly proportional to the power of excitation. Thus, the influence of a non-equilibrium electron-hole plasma (generated by the first pulse) on the efficiency of the THz emission generated by photo-excited charge carriers (excited by the second pulse) can be studied with this experimental setup.

Fig. 2 shows the dependence of THz power on incidence angle for s- and p-optical pulse polarizations.

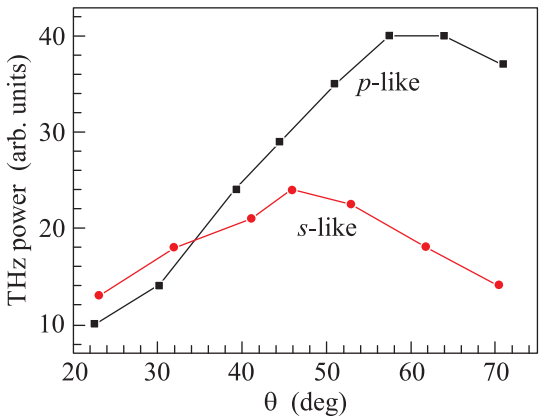

Fig. 2. (Color online) Experimental dependencies of THz power on angle of incidence of excited pulse for s- and p-polarizations. The excitation light wavelength was equal to 730 nm

It can be seen that, for both cases, dependence is not monotonic: the THz power grows with increasing incidence angle, reaches a maximum, and then decreases. For an incident angle of 35 degrees, the intensities have similar values for both polarizations. This result is different from what is observed for bulk GaAs (pure, with an electron concentration $n < 10^{14}\,\mathrm{cm}^3$), where the intensities for the two polarizations differ by factor of two. Such observed behavior differs from the bulk material case [14]. This indicates that, at moderate excitation power, the THz generation process is strongly influenced by light absorption in the NWs.

The NW influence can be further confirmed by studying the dependence of the generated THz power on the excitation pulse photon energy, as shown in Fig. 3. This measurement was carried out in a specular reflec-

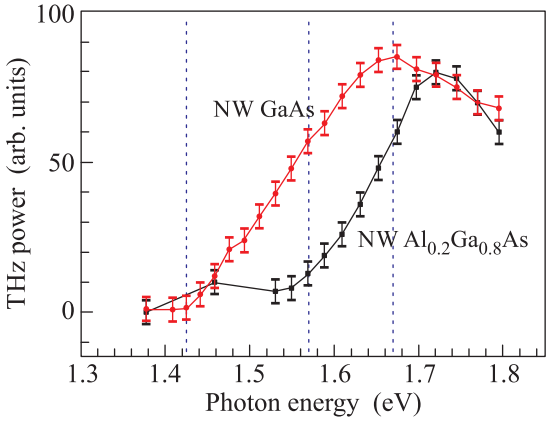

Fig. 3. (Color online) Dependence of THz emission power on a photon energy of the exciting optical pulse taken at incidence angle 45 degrees. The vertical dashed lines define charateristic energy band gap of GaAs ($E_g = 1.424\,\mathrm{eV}$), band gap of $Al_{0.2}Ga_{0.8}As$ ($E_g = 1.67\,\mathrm{eV}$), and the edge of absorption $Al_{0.2}Ga_{0.8}As$ nanowires. The polarization of excitation pulse was p-type

tion geometry with an incident angle of 45 degrees. The similar data for GaAs NWs (the sample F974, see [9]) is also demonstrated in Fig. 3. As one can see, the dependencies have different behavior. For AlGaAs NWs, for photon energy below 1.57 eV, the THz power is about the noise level. On the contrary, the significantly higher power was observed for GaAs NWs, as expected from the bulk GaAs material [18]. With the increase of photon energy above 1.57 eV, the THz power rapidly grows for AlGaAs NWs. The vertical dashed lines on Fig. 3 indicate the band gaps of GaAs (1.424 eV) and $Al_{0.2}Ga_{0.8}As$ (1.67 eV) at room temperature, and the edge of absorption of $Al_{0.2}Ga_{0.8}As$ nanowires. The threshold photon energy of 1.57 eV is about 100 meV lower than the bandgap of $Al_{0.2}Ga_{0.8}As$.

It has been experimentally demonstrated that, in III–V NWs, coexistence of cubic and hexagonal phases occurs [19, 20] and, in such cases, the effective bandgap width can be reduced. Recent photoluminescence studies of NWs with composition $Al_{0.3}Ga_{0.7}As$ and a diameter of about 60 nm have shown that, in such structures, the photoluminescence peak is shifted to a lower energy relative to the band gap of bulk $Al_{0.3}Ga_{0.7}As$, and the value of this shift is approximately 100 meV [21]. The reason for such a shift can be attributed to the structural composition of the NW: it is a mixture of cubic and hexagonal phases. The NWs under study in the present work are similar both in terms of composition and dimensions to those reported in [21] and, therefore, the observed 100 meV reduction in bandgap is reasonable. It is worth noting, that at the same growth rates the composition of Al in NWs is lower compared to AlGaAs two-dimensional layers due to the different kinetics of Al adatom incorporation. This further supports the theory that the NWs are playing a dominant role in the THz generation process relative to the effect of the substrate or wetting layer. With regards to the precise THz generation mechanism it can be noted that the rapid current of photoexcited carriers in a nanowire or crystal may be caused by the drift motion in the electric field of heterojunction, by ambipolar diffusion due to the inhomogeneous excitation or by the anisotropy in the momentum distribution of charge carriers at the metal-semiconductor boundary; or by their combination (the contribution of the drift motion in the contact electric field E_c is seemingly insignificant and it is opposite).

As was pointed out earlier, the dynamics of the charge carriers has crucial importance for application of NWs in electronic and optoelectronic devices. It is evident that non-equilibrium electron-hole plasmas in NWs will affect the THz emission from NWs, and the temporal picture of THz generation will be defined by relaxation and recombination of the charge carriers. Thus, studies of the dynamics of the THz emission provide a powerful tool for, in turn, probing electron and hole dynamics.

Fig. 4 shows the time dynamics of THz radiation from the moment when electron-hole plasma was excited by the first optical pulse. It can be seen that, for zero delay, there is a sharp rise of THz emission power, which peaks at the value corresponding to that measured in the absence of the first excitation pulse. Insets show the detailed temporal dependence in the region of zero delay. On the left inset one can see a small increase in the THz emission at zero delay, as well as its decrease for a delay of about 2 ps. The increase can be caused by the the interference of two THz pulses. But a decrease

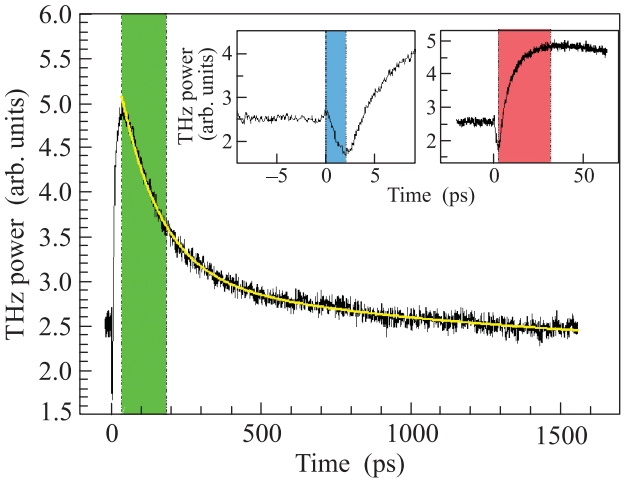

Fig. 4. (Color online) Dependence of the THz power as a function of the delay between two optical excitation pulses. Solid line shows smoothed dependence. Filled area shows "the fast" part (with relaxation time, 130 ps). Insets show the dependences for the small value of the delay (from −10 to 100 ps). The excitation light wavelength was equal to 730 nm. The polarization of excitation pulse was *s*-type. The average power density of the exciting light was equal to 8.8 W/cm^2

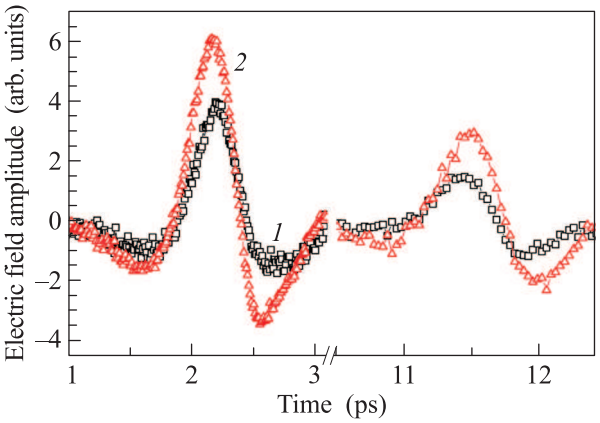

Fig. 5. (Color online) Temporal dependence of THz electric field without non-equilibrium electron-hole plasma (*1*), and with excitation of plasma (*2*). Delay time between first and second excitation pulse is 30 ps. The excitation light wavelength was equal to 750 nm. The polarization of excitation pulse was *p*-type

can be associated with the screening of the electric field E_h by non-equilibrium electrons and holes that are being separated in this field, and also with the possible deceleration of non-equilibrium electrons and holes, which contribute to the THz generation, as the anisotropy in the momentum distribution of charge carriers (generated by first pulse) at the metal-semiconductor boundary and ambipolar diffusion (of the carriers generated by first pulse) form an electric field.

It is not possible to determine the screening time with a good precision as, at the same time, there is a process that results in an increase in THz generation efficiency. This increase can be seen in the right inset of Fig. 4, and takes a time frame of about 30 ps. The increase in the efficiency of THz emission can be explained either: i) by an increase in momentum relaxation time of charge carriers (which leads to an increase in mobility); or ii) by an increase in the lifetime of non-equilibrium charge carriers. For detailed study of the phenomenon, measurements of THz time domain pulse waveforms were made by electro-optic sampling.

Fig. 5 shows temporal dependence of the THz electric field in the case of absence of the first optical excitation pulse, and also the response to excitation by two optical pulses, separated by 30 ps which is when the maximum efficiency of THz emission is achieved. Also that for both cases there are two THz pulses: the main THz pulse and the THz pulse reflected from the backside of the sample. It can be seen that introduction of an additional electron-hole plasma results in the main THz pulse appearing earlier by about 30 fs, whereas the reflected THz pulse is delayed. It should be noted that the temporal shift of THz pulse increases with an increase in the interval between the optical pulses from 0 to 30 ps, reaches maximum and then decreases.

Such a variation in the phase of THz pulse cannot be explained simply by the phase variation during the generation of the THz pulse, which always increases with increasing life time of the charge carriers and decreasing collision rate [22]. However, this result can be explained by the phase variation during transmission of the wave through the boundary between absorbing and non-absorbing media [23]. An electromagnetic wave, when it crosses such a boundary, it acquires the phase φ given by

$$\tan\varphi \approx -\frac{\alpha c\cos\theta}{2\omega(1+n\cos\theta)}, \qquad (1)$$

where α is an absorption coefficient of THz wave with frequency ω, n is a refractive index, θ is an incidence angle, and c is the light velocity. Relation (1) is valid, when $\alpha c/2\omega < n$. The phase is negative, and is defined by quantities α and n, which depend on the momentum relaxation time of the charge carriers p and their concentration. It can be shown that absorption coefficient increases and refractive index decreases with increasing momentum relaxation time, assuming $\omega < 1/\tau_p$, which is the case in our experiments. Thus, the experimental results (the increase of efficiency of THz radiation and

the variation of the THz pulse phase) can be explained by an increase of the momentum relaxation time induced by presence of electron-hole plasma.

The NWs under study are a mixture of cubic and hexagonal phases, and therefore the boundaries between cubic and hexagonal domains may contain defects (non-radiative centres) which can capture electron and holes and therefore reduce the mobility of the charge carriers. Such centres can also be found on the surface of NWs. Thus, the process that leads to an increase in THz generation efficiency is most likely caused by the capture of electrons and holes by non-radiative centres. When such centres become populated by photoexcited electrons and holes, the mobility is increased. As demonstrated by right inset in Fig. 4, where the characteristic capture time is about 10 ps. The subsequent recovery of the original THz generation efficiency consists of two stages. At the first (fast) stage there is a rapid decrease in THz generation efficiency characterised by decay time of 130 ps. For the second (slow) stage the decay time is 1350 ps. Restoration of the initial value of THz efficiency is explained by non-radiative recombination via non-radiative centres and interband radiative recombination. Coexistence of the fast and slow stages of restoration of efficiency of THz emission can be explained by existence of non-radiative centres with different capture cross-sections and different mechanisms of recombination [24].

To conclude, we have investigated the process of THz generation by AlGaAs nanowires illuminated by femtosecond optical pulses. We have shown that THz generation is defined by the photocurrent excited by absorption of light in nanowires. We have demonstrated that the effective band gap in nanowires is reduced by about 100 meV with respect to the bulk due to the coexistence of cubic and hexagonal faces in nanowires. The dynamics of a non-equilibrium electron-hole plasma was studied by the optical pump THz probe method. The creation of an electron-hole mobility plasma in NWs improves the efficiency of THz generation via the capture of charge carriers by non-radiative centers localized on the boundaries between cubic and hexagonal domains, both in the NWs volume and on the NW surface. Recombination of non-equilibrium carriers occurs in two stages: fast recombination of free electrons and holes (with a relaxation time of about 130 ps), and slow recombination (with a relaxation time of about 1350 ps), which involves the capture of electrons and holes on the defects of crystalline structure of nanowires and interband radiative recombination.

The work has been supported by RFBR and by the Program of the Presidium of RAS, and by the FP7 ITN Notedev, FP7 ITN NanoEmbrace, and FP7 IRSES POLATER. The nanowire samples were grown under the support of Russian Science Foundation (Project # 14-12-00393).

1. M. T. Björk, B. J. Ohlsson, C. Thelander, A. I. Persson, K. Deppert, L. R. Wallenberg, and L. Samuelson, Appl. Phys. Lett. **81**, 4458 (2002).
2. X. Duan, Y. Huang, Y. Cui, J. Wang, and C. M. Lieber, Nature **409**, 66 (2001).
3. J. Wang, M. S. Gudiksen, X. Duan, Y. Cui, and C. M. Lieber, Science **293**, 1455 (2001).
4. M. Reid, I. V. Cravetchi, R. Fedosejevs, I. M. Tiginyanu, L. Sirbu, Appl. Phys. Lett. **86**, 021904 (2005).
5. S. He, X. Chen, X. Wu, G. Wang, and F. Zhao, J. Light. Tech. **26**, 1519 (2008).
6. P. Hoyer, M. Theuer, R. Beigang, and E.-B. Kley., Appl. Phys. Lett. **93**, 091106 (2008).
7. D. V. Seletskiy, M. P. Hasselbeck, J. G. Cederberg, A. Katzenmeyer, M. E. Toimil-Molares, F. Leonard, A. A. Talin, and M. Sheik-Bahae, Phys. Rev. B **84**, 115421 (2011).
8. V. N. Trukhin, A. S. Buyskih, A. D. Buravlev, G. E. Cirlin, D. P. Horkov, L. L. Samoilov, and Yu. B. Samsonenko, *Proceedings 37th International Conference on Infrared, Millimeter, and Terahertz Waves* (IRMMW-THz) (2012), DOI:10.1109/IRMMW-THz.2012.6380432.
9. V. N. Trukhin, A. S. Buyskikh, N. A. Kaliteevskaya, A. D. Bourauleuv, L. L. Samoilov, Yu. B. Samsonenko, G. E. Cirlin, M. A. Kaliteevski, and A. J. Gallant, Appl. Phys. Lett. **103**, 072108 (2013).
10. X.-C. Zhang, J. T. Darrow, B. B. Hu, D. H. Auston, M. T. Schmidt, P. Tham, and E. S. Yang, Appl. Phys. Lett. **56**, 2228 (1990).
11. J. E. Pedersen, I. Balslev, J. M. Hvam, and S. R. Keiding., Appl. Phys. Lett. **61**, 1372 (1992).
12. S. L. Chuang, S. Schmitt-Rink, B. I. Greene, P. N. Saeta, and A. F. J. Levi, Phys. Rev. Lett. **68**, 102 (1992).
13. X.-C. Zhang and D. H. Auston, J. Appl. Phys. **71**, 326 (1992).
14. X.-C. Zhang, B. B. Hu, J. T. Darrow, and D. H. Auston, Appl. Phys. Lett. **56**, 1011 (1990).
15. J. N. Heyman, N. Coates, A. Reinhardt, and G. Strasser, Appl. Phys. Lett. **83**, 5476 (2003).
16. V. I. Belinicher and S. M. Ryvkin, JETP **54**, 190 (1981).
17. R. S. Wagner and W. C. Ellis, Appl. Phys. Lett. **4**, 89 (1964).
18. A. Arlauskas and A. Krotkus, Semicond. Sci. Tech. **27**, 115015 (2012).
19. V. G. Dubrovskii, G. E. Cirlin, and V. M. Ustinov, Semiconductors **43**, 1539 (2009).
20. J. Motohisa, J. Takeda, M. Inari, J. Noborisaka, and T. Fukui, Physica E **23**, 298 (2004).

21. V. N. Kats, V. P. Kochereshko, A. V. Platonov, T. V. Chizhova, G. E. Cirlin, A. D. Bouravleuv, Yu. B. Samsonenko, I. P. Soshnikov, E. V. Ubyivovk, J. Bleuse, and H. Mariette, Semicond. Sci. Tech. **27**, 015009 (2012).
22. V. N. Truchin, A. V. Andrianov, and N. N. Zinov'ev, Phys. Rev. B **78**, 155325 (2008).
23. V. N. Trukhin, A. D. Buravlev, V. Dhaka, G. E. Cirlin, I. A. Mustafin, M. A. Kaliteevski, H. Lipsanen, and Yu. B. Samsonenko, Lith. J. Phys. **54**, 41 (2014).
24. V. N. Abakumov, V. I. Perel, and I. N. Yassievich, *Nonradiative Recombination in Semiconductors, Modern Problems in Condensed Matter Sciences*, ed. by V. M. Agranovich and A. A. Maradudin, North-Holland, Amsterdam (1991), v. 33.